$\bar{B} \to X_s\gamma$ in BLMSSM*

Jian-Bin Chen(陈建宾)[1†] Meng Zhang(张梦)[1] Li-Li Xing(邢丽丽)[1‡] Tai-Fu Feng(冯太傅)[2§]
Shu-Min Zhao(赵树民)[2¶] Ke-Sheng Sun(孙科盛)[3♯]

[1]College of Physics and Optoelectronic Engineering, Taiyuan University of Technology, Taiyuan 030024, China
[2]Department of Physics, Hebei University, Baoding, 071002, China
[3]Department of Physics, Baoding University, Baoding, 071000, China

Abstract: Applying the effective Lagrangian method, we study the Flavor Changing Neutral Current $b \to s\gamma$ within the minimal supersymmetric extension of the standard model where baryon and lepton numbers are local gauge symmetries. Constraints on the parameters are investigated numerically with the experimental data on branching ratio of $\bar{B} \to X_s\gamma$. Additionally, we present the corrections to direct CP-violation in $\bar{B} \to X_s\gamma$ and time-dependent CP-asymmetry in $B \to K^*\gamma$. With appropriate assumptions on parameters, we find the direct CP-violation A_{CP} is very small, while one-loop contributions to $S_{K^*\gamma}$ can be significant.

Keywords: BLMSSM, Electroweak radiative corrections, B decay

DOI:

I. INTRODUCTION

Since the Flavor Changing Neutral Current process(FCNC) $b \to s\gamma$ originates only from loop diagrams, it is very sensitive to new physics beyond the Standard Model(SM). The updated average data of inclusive $\bar{B} \to X_s\gamma$ is [1]

$$BR(\bar{B} \to X_s\gamma)_{exp} = (3.32 \pm 0.15) \times 10^{-4}. \quad (1)$$

and the prediction of SM at next-next-to-leading order (NNLO) is[2-4]

$$BR(\bar{B} \to X_s\gamma)_{SM} = (3.40 \pm 0.17) \times 10^{-4}. \quad (2)$$

Though the deviation of SM prediction from experimental results has been almost eliminated in the past few years, it is helpful to constrain parameters of new physics.

The discovery of Higgs boson on Large Hadron Collider(LHC) makes SM the most successful theory in particle physics. Because of the hierarchy problem and missing of gravitational interaction, it is believed that SM is just an effective approximation of a more fundamental theory at higher scale. Among various extensions of SM, supersymmetric models have been studied for decades.

As the simplest extension, the Minimal Supersymmetric Standard Model(MSSM)[5-7] solves the hierarchy problem as well as the instability of Higgs boson by introducing a superpartner for each SM particle. The Lightest Supersymmetric Particle (LSP) within this frmework also provides candidates of dark matter as Weakly Interacting Massive Particles (WIMPs). However the MSSM can not naturely generates tiny neutrino mass which is needed to explain the observation of neutrino oscillation. To acquire neutrino masses, heavy majorana neutrinos are introduced in the seesaw mechanism, which implies that the lepton numbers are broken. Besides, the baryon numbers are also expected to be broken because of the asymmetry of matter-antimatter in the universe. The authors of [8,9] present the so called BLMSSM model in which the baryon and lepton number are local gauged and spontaneously broken at TeV scale. The experimental bounds on proton decay lifetime is the main motivation of

Received 2 February 2020

* Supported by National Natural Science Foundation of China (11805140, 11347185 and 11905002), the Scientific and Technological Innovation Programs of Higher Education Institutions in Shanxi(2017113), Natural Science Foundation of Shanxi Province(201801D221021 and 201801D221031), Natural Science Foundation of Hebei Province(A2020201002), the China Scholarship Council(201906935031)

† E-mail: chenjianbin@tyut.edu.cn
‡ E-mail: xinglili@tyut.edu.cn
§ E-mail: fengtf@hbu.edu.cn
¶ E-mail: zhaosm@hbu.edu.cn
♯ E-mail: sunkesheng@bdu.edu.cn

great desert hypothesis. In BLMSSM, the proton decay can be avoid with discrete symmetry called matter parity and R-parity[10]

To describe the symmetries of baryon and lepton numbers, gauge group is enlarged to $SU(3)_C\otimes SU(2)_L\otimes U(1)_Y\otimes U(1)_B\otimes U(1)_L$. Then corrections to various observations can be induced from new gauge boson and exotic fields within this scenario. In ref. [11], corrections to anomalous magnetic moment from one loop diagrams and two-loop Barr-Zee type diagrams are investigated with effective Lagrangian method. One-loop contributions to $c(t)$ electric dipole moment in CP-Violating BLMSSM is presented in ref. [12]. To account for the experimental data on Higgs, the authors of [13] study the signals of $h\to\gamma\gamma$ and $h\to VV^*(V=Z,W)$ with a 125 GeV Higgs. In this work, we use the branching ratio to constrain the parameters. Furthermore, we present the corrections to CP-Violation of $b\to s\gamma$ due to new parameters introduced in this model.

Our presentation is organized as follows. In section II, we briefly introduce the construction of BLMSSM and the interactions we need for our caculation. After that, we present the one-loop corrections to branching ratio and CP-Violation with effective Lagrangian method in section III. Numerical results are discussed in section IV and the conclusions is given in section V.

II. INTRODUCTION TO BLMSSM

The BLMSSM is based on gauge symmetry $SU(3)_C\otimes SU(2)_L\otimes U(1)_Y\otimes U(1)_B\otimes U(1)_L$. In order to cancel the anomalies of Baryon number(B), exotic quarks $\hat{Q}_4\sim(3,2,1/6,B_4,0),\hat{U}_4^c\sim(\bar{3},1,-2/3,-B_4,0),\hat{D}_4^c\sim(\bar{3},1,1/3,-B_4,0),\hat{Q}_5^c\sim(\bar{3},2,-1/6,-(1+B_4),0),\hat{U}_5\sim(3,1,2/3,1+B_4,0),\hat{D}_5\sim(3,1,-1/3,1+B_4,0)$ are introduced. Baryon number are broken spontaneously after Higgs superfields $\hat{\Phi}_B\sim(1,1,0,1,0),\hat{\varphi}_B\sim(1,1,0,-1,0)$ acquire nonzero vacuum expectation values(VEVs). To deal with the anomalies of Lepton number(L), exotic leptons $\hat{L}_4\sim(1,2,-1/2,0,L_4),\hat{E}_4^c\sim(1,1,1,0,-L_4),\hat{N}_4^c\sim(1,1,0,0,-L_4),\hat{L}_5^c\sim(1,2,1/2,0,-(3+L_4)),\hat{E}_5\sim(1,1,-1,0,3+L_4),\hat{N}_5\sim(1,1,0,0,3+L_4)$ are introduced, and $\hat{\Phi}_L\sim(1,1,0,0,-2),\hat{\varphi}_L\sim(1,1,0,0,2)$ are responsable for the breaking of lepton number[9]. The superfields $\hat{X}\sim(1,1,0,2/3+B_4,0),\hat{X}'\sim(1,1,0,-(2/3+B_4),0)$ which mediate the decay of exotic quarks are added in this model to avoid their stability.

Given the superfields above, one can construct the superpotential as

$$\mathcal{W}_{BLMSSM}=\mathcal{W}_{MSSM}+\mathcal{W}_B+\mathcal{W}_L+\mathcal{W}_X, \tag{3}$$

where $\mathcal{W}_{MSSM}$ indicates the superpotential of MSSM, and

$$\begin{aligned}
\mathcal{W}_B=&\lambda_Q\hat{Q}_4\hat{Q}_5^c\hat{\Phi}_B+\lambda_U\hat{U}_4^c\hat{U}_5\hat{\varphi}_B+\lambda_D\hat{D}_4^c\hat{D}_5\hat{\varphi}_B+\mu_B\hat{\Phi}_B\hat{\varphi}_B\\
&+Y_{u_4}\hat{Q}_4\hat{H}_u\hat{U}_4^c+Y_{d_4}\hat{Q}_4\hat{H}_d\hat{D}_4^c+Y_{u_5}\hat{Q}_5^c\hat{H}_d\hat{U}_5+Y_{d_5}\hat{Q}_5^c\hat{H}_u\hat{D}_5,\\
\mathcal{W}_L=&Y_{e_4}\hat{L}_4\hat{H}_d\hat{E}_4^c+Y_{\nu_4}\hat{L}_4\hat{H}_u\hat{N}_4^c+Y_{e_5}\hat{L}_5^c\hat{H}_u\hat{E}_5+Y_{\nu_5}\hat{L}_5^c\hat{H}_d\hat{N}_5\\
&+Y_\nu\hat{L}\hat{H}_u\hat{N}^c+\lambda_{N^c}\hat{N}^c\hat{N}^c\hat{\varphi}_L+\mu_L\hat{\Phi}_L\hat{\varphi}_L,\\
\mathcal{W}_X=&\lambda_1\hat{Q}\hat{Q}_5^c\hat{X}+\lambda_2\hat{U}^c\hat{U}_5\hat{X}'+\lambda_3\hat{D}^c\hat{D}_5\hat{X}'+\mu_X\hat{X}\hat{X}'.
\end{aligned} \tag{4}$$

The soft breaking terms are given by

$$\begin{aligned}
\mathcal{L}_{soft}=&\mathcal{L}_{soft}^{MSSM}-(m_{\tilde{N}^c}^2)_{IJ}\tilde{N}_I^{c*}\tilde{N}_J^c-m_{\tilde{Q}_4}^2\tilde{Q}_4^\dagger ger\tilde{Q}_4-m_{\tilde{U}_4}^2\tilde{U}_4^{c*}\tilde{U}_4^c-m_{\tilde{D}_4}^2\tilde{D}_4^{c*}\tilde{D}_4^c-m_{\tilde{Q}_5}^2\tilde{Q}_5^{c\dagger}\tilde{Q}_5^c-m_{\tilde{U}_5}^2\tilde{U}_5^*\tilde{U}_5-m_{\tilde{D}_5}^2\tilde{D}_5^*\tilde{D}_5-m_{\tilde{L}_4}^2\tilde{L}_4^\dagger ger\tilde{L}_4-M_{\tilde{\nu}_4}^2\tilde{\nu}_4^{c*}\tilde{\nu}_4^c\\
&-m_{\tilde{E}_4}^2\tilde{e}_4^{c*}\tilde{e}_4^c-m_{\tilde{L}_5}^2\tilde{L}_5^{c\dagger}\tilde{L}_5^c-M_{\tilde{\nu}_5}^2\tilde{\nu}_5^*\tilde{\nu}_5-m_{\tilde{E}_5}^2\tilde{e}_5^*\tilde{e}_5-m_{\Phi_B}^2\Phi_B^*\Phi_B-m_{\varphi_B}^2\varphi_B^*\varphi_B-m_{\Phi_L}^2\Phi_L^*\Phi_L-m_{\varphi_L}^2\varphi_L^*\varphi_L-(m_B\lambda_B\lambda_B+m_L\lambda_L\lambda_L+h.c.)\\
&+\left\{A_{u_4}Y_{u_4}\tilde{Q}_4H_u\tilde{U}_4^c+A_{d_4}Y_{d_4}\tilde{Q}_4H_d\tilde{D}_4^c+A_{u_5}Y_{u_5}\tilde{Q}_5^cH_d\tilde{U}_5+A_{d_5}Y_{d_5}\tilde{Q}_5^cH_u\tilde{D}_5+A_{BQ}\lambda_Q\tilde{Q}_4\tilde{Q}_5^c\Phi_B+A_{BU}\lambda_U\tilde{U}_4^c\tilde{U}_5\varphi_B+A_{BD}\lambda_D\tilde{D}_4^c\tilde{D}_5\varphi_B\right.\\
&\left.+B_B\mu_B\Phi_B\varphi_B+h.c.\right\}+\left\{A_{e_4}Y_{e_4}\tilde{L}_4H_d\tilde{E}_4^c+A_{N_4}Y_{N_4}\tilde{L}_4H_u\tilde{N}_4^c+A_{e_5}Y_{e_5}\tilde{L}_5^cH_u\tilde{E}_5+A_{N_5}Y_{\nu_5}\tilde{L}_5^cH_d\tilde{N}_5+A_NY_N\tilde{L}H_u\tilde{N}^c\right.\\
&\left.+A_{N^c}\lambda_{N^c}\tilde{N}^c\tilde{N}^c\varphi_L+B_L\mu_L\Phi_L\varphi_L+h.c.\right\}+\left\{A_1\lambda_1\tilde{Q}\tilde{Q}_5^cX+A_2\lambda_2\tilde{U}^c\tilde{U}_5X'+A_3\lambda_3\tilde{D}^c\tilde{D}_5X'+B_X\mu_XXX'+h.c.\right\}.
\end{aligned} \tag{5}$$

The first term $\mathcal{L}_{soft}^{MSSM}$ denotes the soft breaking terms of MSSM. To break the gauge symmetry from $SU(3)_C\otimes SU(2)_L\otimes U(1)_Y\otimes U(1)_B\otimes U(1)_L$ to electromagnetic symmetry $U(1)_e$, nonzero VEVs v_u,v_d and $v_B,\bar{v}_B,v_L,\bar{v}_L$ are allocated to $SU(2)_L$ doublets H_u,H_d and $SU(2)_L$ singlets $\Phi_B,\varphi_B,\Phi_L,\varphi_L$.

$$\begin{aligned}
H_u=&\begin{pmatrix}H_u^+\\(v_u+H_u^0+iP_u^0)/\sqrt{2}\end{pmatrix},\\
H_u=&\begin{pmatrix}(v_d+H_d^0+iP_d^0)/\sqrt{2}\\H_d^-\end{pmatrix},\\
\Phi_B=&(v_B+\Phi_B^0+iP_B^0)/\sqrt{2},\\
\varphi_B=&(\bar{v}_B+\varphi_B^0+i\bar{P}_B^0)/\sqrt{2},\\
\Phi_L=&(v_L+\Phi_L^0+iP_L^0)/\sqrt{2},\\
\varphi_L=&(\bar{v}_L+\varphi_L^0+i\bar{P}_L^0)/\sqrt{2}.
\end{aligned} \tag{6}$$

Here we take the notation $\tan\beta=v_u/v_d,\tan\beta_B=\bar{v}_B/v_B$

and $\tan\beta_L = \bar{v}_L/v_L$. After spontaneously breaking and unitary transformation from interactive eigenstate to mass eigenstate, one can extract the Feynman rules and mass spectrums in BLMSSM. The mass matrices of the particles that mediate the one-loop process $b \to s\gamma$ can be found in ref. [14]. The Feynman rules that we need can be extracted from the following terms, where all the repeated index of generation should be summed over.

$$\begin{aligned}
\mathcal{L}_{H^+du} =& \left(-Y_d^I Z_H^{1i} P_L + Y_u^J Z_H^{2i} P_R\right) K^{JI*} \bar{d}^I u^J H_i^-,\\
\mathcal{L}_{\tilde{D}\chi^0 d} =& \left[\left(\frac{-e}{\sqrt{2}s_W c_W} Z_D^{Ii}\left(\frac{1}{3}Z_N^{1j} s_W - Z_N^{2j} c_W\right) + Y_d^I Z_D^{(I+3)i} Z_N^{3j}\right) P_L\right.\\
&\left. + \left(\frac{-e\sqrt{2}}{3c_W} Z_D^{(I+3)i} Z_N^{1j*} + Y_d^I Z_D^{Ii} Z_N^{3j*}\right) P_R\right] \bar{\chi}_j^0 d^I \tilde{D}_i^+,\\
\mathcal{L}_{\tilde{D}\chi_B^0 d} =& \frac{\sqrt{2}}{3} g_B \left(Z_{N_B}^{1j} Z_D^{Ii} P_L + Z_{N_B}^{1j*} Z_D^{(I+3)i} P_R\right) \bar{\chi}_{B_j}^0 d^I \tilde{D}^+,\\
\mathcal{L}_{\tilde{U}\chi^- d} =& \left[\left(\frac{-e}{s_W} Z_U^{Ji*} Z_+^{1j} + Y_u^J Z_U^{(J+3)i*} Z_+^{2j}\right) P_L - Y_d^I Z_U^{Ji*} Z_-^{2j*} P_R\right]\\
&\times K^{JI} \bar{\chi}^- d \tilde{U}^-,\\
\mathcal{L}_{Xb'd} =& \left[\lambda_1 (W_b^\dagger)_{j1} (Z_X)_{1k} P_L - \lambda_3^* (U_b^\dagger)_{j2} (Z_X)_{2k} P_R\right] \bar{b}'_j d^I X_k,\\
\mathcal{L}_{\tilde{b}'\tilde{X}d} =& -\left[\lambda_1 (W_{\tilde{b}'}^*)_{3\rho} P_L + \lambda_3^* (W_{\tilde{b}'})_{4\rho} P_R\right] \bar{\tilde{X}} d^I \tilde{b}'_\rho,\\
\mathcal{L}_{\tilde{D}\Lambda_G d} =& g_3 \sqrt{2} Y_{\alpha\beta}^a \left(-Z_D^{Ii} P_L + Z_D^{(I+3)i} P_R\right) \bar{\Lambda}_G^a d_\beta^I \tilde{D}_{i\alpha}^+.
\end{aligned} \tag{7}$$

The interactions from MSSM are collected from ref. [7] for completeness, and the Feynman gauge are adopt in our derivation to keep consist with the MSSM sector.

III. ONE-LOOP CORRECTIONS TO $b \to s\gamma$ FROM BLMSSM

The flavor transition process $b \to s\gamma$ can be described by effective Hamiltonian at scale $\mu = O(m_b)$ as follow [15-17]:

$$\begin{aligned}
\mathcal{H}_{eff}(b \to s\gamma) =& -\frac{4G_F}{\sqrt{2}} V_{ts}^* V_{tb} \left[C_1 Q_1^c + C_2 Q_2^c\right.\\
&\left. + \sum_{i=3}^{6} C_i Q_i + \sum_{i=7}^{8} (C_i Q_i + \tilde{C}_i \tilde{Q}_i)\right],
\end{aligned} \tag{8}$$

and the operators are given by ref. [18-22]:

$$\begin{aligned}
O_1^c =& (\bar{s}_L \gamma_\mu T^a b_L)(\bar{c}_L \gamma^\mu T^a b_L),\\
O_2^c =& (\bar{s}_L \gamma_\mu b_L)(\bar{c}_L \gamma^\mu T^a b_L),\\
O_3 =& (\bar{s}_L \gamma_\mu b_L) \sum_q (\bar{q}\gamma^\mu q),\\
O_4 =& (\bar{s}_L \gamma_\mu T^a b_L) \sum_q (\bar{q}\gamma^\mu T^a q),\\
O_5 =& (\bar{s}_L \gamma_\mu \gamma_\nu \gamma_\rho b_L) \sum_q (\bar{q}\gamma^\mu \gamma^\mu \gamma^\nu \gamma^\rho q),\\
O_6 =& (\bar{s}_L \gamma_\mu \gamma_\nu \gamma_\rho T^a b_L) \sum_q (\bar{q}\gamma^\mu \gamma^\mu \gamma^\nu \gamma^\rho T^a q),\\
O_7 =& e/g_s^2 m_b (\bar{s}_L \sigma_{\mu\nu} b_R) F^{\mu\nu},\\
O_8 =& 1/g_s^2 m_b (\bar{s}_L \sigma_{\mu\nu} T^a b_R) G^{a,\mu\nu},\\
\tilde{O}_7 =& e/g_s^2 m_b (\bar{s}_R \sigma_{\mu\nu} b_L) F^{\mu\nu},\\
\tilde{O}_8 =& 1/g_s^2 m_b (\bar{s}_R \sigma_{\mu\nu} T^a b_L) G^{a,\mu\nu}.
\end{aligned} \tag{9}$$

Coefficients of these operators can be extracted from Feynman amplitudes that originate from considered diagrams. Actually only the Coefficients of $O_{7,8}$ and $\tilde{O}_{7,8}$ are needed if we adopt the branching ratio formula presented in ref. [15]:

$$\begin{aligned}
BR(\bar{B} \to X_s\gamma)_{NP} =& 10^{-4} \times \left\{(3.32 \pm 0.15)\right.\\
&+ \frac{16\pi^2 a_{77}}{\alpha_s^2(\mu_b)} [|C_{7,NP}(\mu_{EW})|^2 + |\tilde{C}_{7,NP}(\mu_{EW})|^2]\\
&+ \frac{16\pi^2 a_{88}}{\alpha_s^2(\mu_b)} [|C_{8,NP}(\mu_{EW})|^2 + |\tilde{C}_{8,NP}(\mu_{EW})|^2]\\
&+ \frac{4\pi}{\alpha_s(\mu_b)} \mathrm{Re}[a_7 C_{7,NP}(\mu_{EW}) + a_8 C_{8,NP}(\mu_{EW})\\
&+ \frac{4\pi a_{78}}{\alpha_s(\mu_b)} (C_{7,NP}(\mu_{EW}) C_{8,NP}(\mu_{EW})\\
&\left.\left. + \tilde{C}_{7,NP}(\mu_{EW}) \tilde{C}_{8,NP}(\mu_{EW}))\right]\right\},
\end{aligned} \tag{10}$$

where the first term is SM prediction. The others come from new physics in which $C_{7,NP}(\mu_{EW})$, $C_{8,NP}(\mu_{EW})$, $\tilde{C}_{7,NP}(\mu_{EW})$ and $\tilde{C}_{8,NP}(\mu_{EW})$ indicate Wilson coefficients at electroweak scale. It is an advantage of this expression that we don't have to evolve them down to hadronic scale $\mu \sim m_b$ as the effect of evolution has already been involved in the coefficients $a_{7,8,77,88,78}$. The numerical values of these coefficients are given in table 1.

To obtain the New Physics corrections in BLMSSM, we investigate one-loop diagrams shown in Figure 1. Photons should be attached to all inner lines with electric charge to complete the diagrams of $b \to s\gamma$ that contribute to O_7 and $\tilde{O}_7$. Similarly, diagrams of $b \to sg$ can be

Table 1. Numerical values for the coefficients $a_{7,8,77,88,78}$ at electroweak scale

a_7	a_8	a_{77}	a_{88}	a_{78}
$-7.184 + 0.612i$	$-2.225 - 0.557i$	4.743	0.789	$2.454 - 0.884i$

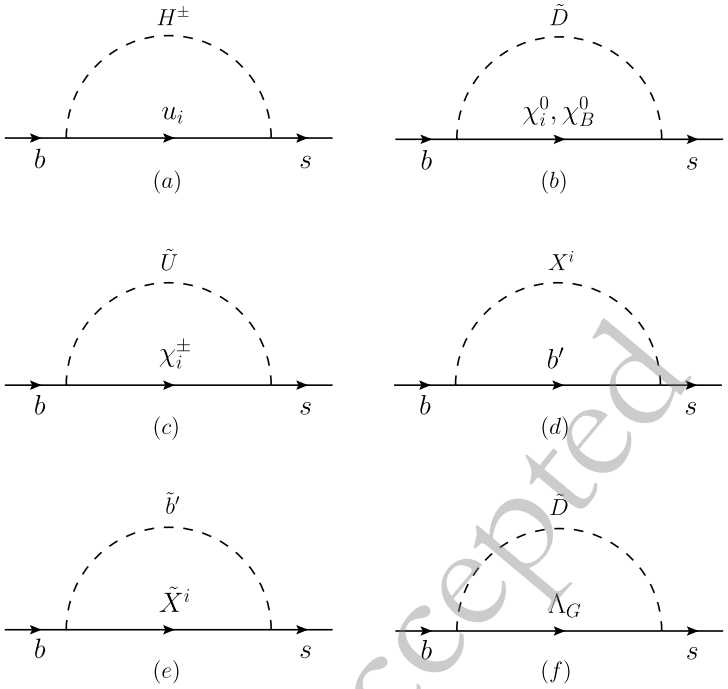

Fig. 1. One-loop Feynman diagrams of $b \to s$. The inner-line particles χ_B^0, X denote baryon neutralinos and new scalar particle introduced in BLMSSM. b' and $\tilde{b}'$ are exotic quarks and squarks respectively. The photon and gluon can be attached in all possible ways

completed with gluons attached to all the inner lines with color charge, and O_8 and $\tilde{O}_8$ originate from these process.

The so-called flavor-changing self-energy diagrams in which photos or gluons are attached to external b or s quarks are not included during our calculations. As studied in Ref. [23-25], the contributions from those self-energy diagrams vanish when one of the external legs is on its mass shell. To preserve the Ward-Takahashi identity during the renormalization of $\bar{s}bg$ and $\bar{s}b\gamma$ vertices, one can always imposing the renormalized self-energies are zero as both b and s are on mass shell.

In details, we attach a photon to SM quark $u_i, (i = 1,2,3)$ or charged Higgs $H^{\pm}$ in Figure 1.(a) to get a set of trigonal diagrams for $b \to s\gamma$, while gluon can only be attached to up-type quarks u_i to form a specific diagram of $b \to sg$. To give a complete correction originating from Figure 1.(a), contributions from all generations of u_i and Higgs should be summed over. From the amplitudes of these diagrams, one can extract Wilson coefficients of electric- and chromomagnetic-dipole operators O_7 and $\tilde{O}_7$ at electroweak scale,

$$\begin{aligned}\frac{G_F}{\sqrt{2}}C_{7\gamma}^{a}(\Lambda) =& -i\Lambda^{-2}(V_{ts}^{*}V_{tb})^{-1}\Big\{(\eta_{H^{\pm}}^{L})_{su_i}^{\dagger}(\eta_{H^{\pm}}^{L})_{u_ib}F_{1,\gamma}^{(a)}(x_{u_i},x_{H^{\pm}})\\ &+\frac{m_f}{m_b}(\eta_{H^{\pm}}^{L})_{su_i}^{\dagger}(\eta_{H^{\pm}}^{R})_{u_ib}F_{2,\gamma}^{(a)}(x_{u_i},x_{H^{\pm}})\Big\},\\ \frac{G_F}{\sqrt{2}}\tilde{C}_{7\gamma}^{a}(\Lambda) =& \frac{G_F}{\sqrt{2}}C_{7\gamma}^{a}(\Lambda)(\eta_{H^{\pm}}^{L}\leftrightarrow\eta_{H^{\pm}}^{R}),\end{aligned} \tag{11}$$

where $x_i = m_i^2/\mu_{EW}^2$. The concrete expressions of relevant couplings are already given in previous section. To be clear, the absence of divergences in the Wilson coefficients associated with one-loop triangle diagrams can be certified by expanding all the propagators in power of $1/(q^2 - m_{f,S}^2)$, where q denotes the loop momentum. It can found that the order of q that appear in denominators are always higher than those in numerators. Thus, we do not have to deal with divergences during our evaluation. The form factors in Eq. (11) can be written as

$$\begin{aligned}F_{1,\gamma}^{(a)}(x,y) =& \left[\frac{1}{72}\frac{\partial^3\varrho_{3,1}}{\partial y^3}+\frac{1}{24}\frac{\partial^2\varrho_{2,1}}{\partial y^2}-\frac{1}{6}\frac{\partial\varrho_{1,1}}{\partial y}\right](x,y),\\ F_{2,\gamma}^{(a)}(x,y) =& \left[\frac{1}{12}\frac{\partial^2\varrho_{2,1}}{\partial y^2}-\frac{1}{6}\frac{\partial\varrho_{1,1}}{\partial y}-\frac{1}{3}\frac{\partial\varrho_{1,1}}{\partial x}\right](x,y),\end{aligned} \tag{12}$$

where function $\varrho_{m,n}(x,y)$ is defined as:

$$\varrho_{m,n}(x,y) = \frac{x^m\ln^n x - y^m\ln^n y}{x-y}. \tag{13}$$

Corrections from all the other diagrams to $C_{7\gamma}$ and $\tilde{C}_{7\gamma}$ can be obtained similarly. In Figure 1.(b), the photon can only be attached to charged $-1/3$ squark $\tilde{D}$. We present contributions from both neutralinos χ_i^0 and baryon neutralinos χ_B^0 at electroweak scale as

$$\begin{aligned}\frac{G_F}{\sqrt{2}}C^b_{7\gamma}(\Lambda)=&-i\Lambda^{-2}(V^*_{ts}V_{tb})^{-1}\Big\{(\xi^L_{\chi^0_i})^\dagger_{s\tilde{D}}(\xi^L_{\chi^0_i})_{\tilde{D}b}F^{(b)}_{1,\gamma}(x_{\chi^0_i},x_{\tilde{D}})\\&+\frac{m_f}{m_b}(\xi^L_{\chi^0_i})^\dagger_{s\tilde{D}}(\xi^R_{\chi^0_i})_{\tilde{D}b}F^{(b)}_{2,\gamma}(x_{\chi^0_i},x_{\tilde{D}})\\&+(\xi^L_{\chi^0_B})^\dagger_{s\tilde{D}}(\xi^L_{\chi^0_B})_{\tilde{D}b}F^{(b)}_{1,\gamma}(x_{\chi^0_B},x_{\tilde{D}})\\&+\frac{m_f}{m_b}(\xi^L_{\chi^0_B})^\dagger_{s\tilde{D}}(\xi^R_{\chi^0_B})_{\tilde{D}b}F^{(b)}_{2,\gamma}(x_{\chi^0_B},x_{\tilde{D}})\Big\},\\\frac{G_F}{\sqrt{2}}\tilde{C}^b_{7\gamma}(\Lambda)=&\frac{G_F}{\sqrt{2}}C^b_{7\gamma}(\Lambda)(\xi^L_{\chi^0_i}\leftrightarrow\xi^R_{\chi^0_i}\,,\,\xi^L_{\chi^0_B}\leftrightarrow\xi^R_{\chi^0_B}).\end{aligned}\tag{14}$$

$$\begin{aligned}F^{(b)}_{1,\gamma}(x,y)=&\left[-\frac{1}{72}\frac{\partial^3\varrho_{3,1}}{\partial^3 y}+\frac{1}{24}\frac{\partial^2\varrho_{2,1}}{\partial^2 y}\right](x,y),\\F^{(b)}_{2,\gamma}(x,y)=&\left[-\frac{1}{12}\frac{\partial^2\varrho_{2,1}}{\partial^2 y}+\frac{1}{6}\frac{\partial\varrho_{1,1}}{\partial y}\right](x,y).\end{aligned}\tag{15}$$

With the photon attached to the charged +2/3 squarks $\tilde{U}$ or chargino $\chi^\pm_i$ in Figure 1.(c), the contributions to Wilson coefficients read

$$\begin{aligned}\frac{G_F}{\sqrt{2}}C^c_{7\gamma}(\Lambda)=&-i\Lambda^{-2}(V^*_{ts}V_{tb})^{-1}\Big\{(\eta^L_{\tilde{U}})^\dagger_{s\chi^\pm_i}(\eta^L_{\tilde{U}})_{\chi^\pm_i b}F^{(c)}_{1,\gamma}(x_{\chi^\pm_i},x\\&+\frac{m_f}{m_b}(\eta^L_{\tilde{U}})^\dagger_{s\chi^\pm_i}(\eta^R_{\tilde{U}})_{\chi^\pm_i b}F^{(c)}_{2,\gamma}(x_{\chi^\pm_i},x_{\tilde{U}})\Big\},\\\frac{G_F}{\sqrt{2}}\tilde{C}^c_{7\gamma}(\Lambda)=&\frac{G_F}{\sqrt{2}}C^c_{7\gamma}(\Lambda)(\eta^L_{\tilde{U}}\leftrightarrow\eta^R_{\tilde{U}}).\end{aligned}\tag{16}$$

$$\begin{aligned}F^{(c)}_{1,\gamma}(x,y)=&\left[-\frac{1}{72}\frac{\partial^3\varrho_{3,1}}{\partial^3 y}+\frac{1}{6}\frac{\partial^2\varrho_{2,1}}{\partial^2 y}-\frac{1}{4}\frac{\partial\varrho_{1,1}}{\partial y}\right](x,y),\\F^{(c)}_{2,\gamma}(x,y)=&\left[-\frac{1}{12}\frac{\partial^2\varrho_{2,1}}{\partial^2 y}+\frac{1}{6}\frac{\partial\varrho_{1,1}}{\partial y}-\frac{1}{2}\frac{\partial\varrho_{1,1}}{\partial x}\right](x,y).\end{aligned}\tag{17}$$

The intermediate particles in Figure 1.(d) are the exotic quarks b' with charge -1/3 and superfield X introduced in BLMSSM. The contributions from this diagram are

$$\begin{aligned}\frac{G_F}{\sqrt{2}}C^d_{7\gamma}(\Lambda)=&-i\Lambda^{-2}(V^*_{ts}V_{tb})^{-1}\Big\{(\eta^L_{X^j})^\dagger_{sb'}(\eta^L_{X^j})_{b'b}F^{(d)}_{1,\gamma}(x_{b'},x_{X^j})\\&+\frac{m_f}{m_b}(\eta^L_{X^j})^\dagger_{sb'}(\eta^R_{X^j})_{b'b}F^{(d)}_{2,\gamma}(x_{b'},x_{X^j})\Big\},\\\frac{G_F}{\sqrt{2}}\tilde{C}^d_{7\gamma}(\Lambda)=&\frac{G_F}{\sqrt{2}}C^d_{7\gamma}(\Lambda)(\eta^L_{X^j}\leftrightarrow\eta^R_{X^j}).\end{aligned}\tag{18}$$

Correspondingly, the corrections of exotic squarks $\tilde{b}'$ with charge -1/3 and fermionic particle X can be obtained from Figure 1.(e)

$$\begin{aligned}\frac{G_F}{\sqrt{2}}C^e_{7\gamma}(\Lambda)=&-i\Lambda^{-2}(V^*_{ts}V_{tb})^{-1}\\&\times\Big\{(\eta^L_{\tilde{b}'})^\dagger_{s\tilde{X}^j}(\eta^L_{\tilde{b}'})_{\tilde{X}^j b}F^{(e)}_{1,\gamma}(x_{\tilde{X}^j},x_{\tilde{b}'})\\&+\frac{m_f}{m_b}(\eta^L_{\tilde{b}'})^\dagger_{s\tilde{X}^j}(\eta^R_{\tilde{b}'})_{\tilde{X}^j b}F^{(e)}_{2,\gamma}(x_{\tilde{X}^j},x_{\tilde{b}'})\Big\},\\\frac{G_F}{\sqrt{2}}\tilde{C}^e_{7\gamma}(\Lambda)=&\frac{G_F}{\sqrt{2}}C^e_{7\gamma}(\Lambda)(\eta^L_{\tilde{b}'}\leftrightarrow\eta^R_{\tilde{b}'}).\end{aligned}\tag{19}$$

$$\begin{aligned}F^{(e)}_{1,\gamma}(x,y)=&\left[-\frac{1}{72}\frac{\partial^3\varrho_{3,1}}{\partial^3 y}+\frac{1}{24}\frac{\partial^2\varrho_{2,1}}{\partial^2 y}\right](x,y),\\F^{(e)}_{2,\gamma}(x,y)=&\left[-\frac{1}{12}\frac{\partial^2\varrho_{2,1}}{\partial^2 y}+\frac{1}{6}\frac{\partial\varrho_{1,1}}{\partial y}\right](x,y).\end{aligned}\tag{20}$$

From Figure 1.(f), we obtain the corrections from gluinos Λ_G in MSSM, the Wilson coefficients at μ_{EW} are

$$\begin{aligned}\frac{G_F}{\sqrt{2}}C^f_{7\gamma}(\Lambda)=&-i\Lambda^{-2}(V^*_{ts}V_{tb})^{-1}\\&\times\Big\{(\eta^L_{\tilde{D}})^\dagger_{s\Lambda_G}(\eta^L_{\tilde{D}})_{\Lambda_G b}F^{(f)}_{1,\gamma}(x_{\Lambda_G},x_{\tilde{D}})\\&+\frac{m_f}{m_b}(\eta^L_{\tilde{D}})^\dagger_{s\Lambda_G}(\eta^R_{\tilde{D}})_{\Lambda_G b}F^{(f)}_{2,\gamma}(x_{\Lambda_G},x_{\tilde{D}})\Big\},\\\frac{G_F}{\sqrt{2}}\tilde{C}^f_{7\gamma}(\Lambda)=&\frac{G_F}{\sqrt{2}}C^f_{7\gamma}(\Lambda)(\eta^L_{\tilde{D}}\leftrightarrow\eta^R_{\tilde{D}}).\end{aligned}\tag{21}$$

with

$$\begin{aligned}F^{(f)}_{1,\gamma}(x,y)=&\left[\frac{1}{24}\frac{\partial^3\varrho_{3,1}}{\partial^3 y}-\frac{1}{8}\frac{\partial^2\varrho_{2,1}}{\partial^2 y}\right](x,y),\\F^{(f)}_{2,\gamma}(x,y)=&\left[\frac{1}{4}\frac{\partial^2\varrho_{2,1}}{\partial^2 y}-\frac{1}{2}\frac{\partial\varrho_{1,1}}{\partial y}\right](x,y).\end{aligned}\tag{22}$$

The corrections to C_{8g} and $\tilde{C}_{8g}$ at electroweak scale can be obtained by attaching the gluon to intermediate virtual particles with colors. For diagrams in Figure 1, the gluon can be attached to SM up-type quarks u_i, squarks in MSSM $\tilde{U},\tilde{D}$, exotic quarks b' with charge -1/3 and its supersymmetric partners $\tilde{b}'$, as well as the gluinos Λ_G. Wilson coefficients at electroweak scale can be formulated as:

$$
\begin{aligned}
&\frac{G_F}{\sqrt{2}}C^a_{8G}(\Lambda) = -i\Lambda^{-2}(V^*_{ts}V_{tb})^{-1}\left\{(\eta^L_{H^\pm})^\dagger_{su_i}(\eta^L_{H^\pm})_{u_ib}F^{(a)}_{1,g}(x_{u_i},x_{H^\pm}) + \frac{m_f}{m_b}(\eta^L_{H^\pm})^\dagger_{su_i}(\eta^R_{H^\pm})_{u_ib}F^{(a)}_{2,g}(x_{u_i},x_{H^\pm})\right\},\\
&\frac{G_F}{\sqrt{2}}\tilde{C}^a_{8G}(\Lambda) = \frac{G_F}{\sqrt{2}}C^a_{8G}(\Lambda)(\eta^L_{H^\pm}\leftrightarrow\eta^R_{H^\pm},\ \eta^L_{G^\pm}\leftrightarrow\eta^R_{G^\pm}),\\
&\frac{G_F}{\sqrt{2}}C^b_{8G}(\Lambda) = -i\Lambda^{-2}(V^*_{ts}V_{tb})^{-1}\left\{(\xi^L_{\chi^0_i})^\dagger_{s\tilde{D}}(\xi^L_{\chi^0_i})_{\tilde{D}b}F^{(b)}_{1,g}(x_{\chi^0_i},x_{\tilde{D}}) + \frac{m_f}{m_b}(\xi^L_{\chi^0_i})^\dagger_{s\tilde{D}}(\xi^R_{\chi^0_i})_{\tilde{D}b}F^{(b)}_{2,g}(x_{\chi^0_i},x_{\tilde{D}})\right.\\
&\qquad\left.+(\xi^L_{\chi^0_B})^\dagger_{s\tilde{D}}(\xi^L_{\chi^0_B})_{\tilde{D}b}F^{(b)}_{1,g}(x_{\chi^0_B},x_{\tilde{D}}) + \frac{m_f}{m_b}(\xi^L_{\chi^0_B})^\dagger_{s\tilde{D}}(\xi^R_{\chi^0_B})_{\tilde{D}b}F^{(b)}_{2,g}(x_{\chi^0_B},x_{\tilde{D}})\right\},\\
&\frac{G_F}{\sqrt{2}}\tilde{C}^b_{8G}(\Lambda) = \frac{G_F}{\sqrt{2}}C^b_{8g}(\Lambda)(\xi^L_{\chi^0_i}\leftrightarrow\xi^R_{\chi^0_i},\ \xi^L_{\chi^0_B}\leftrightarrow\xi^R_{\chi^0_B}),\\
&\frac{G_F}{\sqrt{2}}C^c_{8G}(\Lambda) = -i\Lambda^{-2}(V^*_{ts}V_{tb})^{-1}\left\{(\xi^L_{\chi^\pm_i})^\dagger_{s\tilde{D}}(\xi^L_{\chi^\pm_i})_{\tilde{D}b}F^{(c)}_{1,g}(x_{\chi^\pm_i},x_{\tilde{U}}) + \frac{m_f}{m_b}(\xi^L_{\chi^\pm_i})^\dagger_{s\tilde{D}}(\xi^R_{\chi^\pm_i})_{\tilde{D}b}F^{(c)}_{2,g}(x_{\chi^\pm_i},x_{\tilde{U}})\right\},\\
&\frac{G_F}{\sqrt{2}}\tilde{C}^c_{8G}(\Lambda) = \frac{G_F}{\sqrt{2}}C^c_{8g}(\Lambda)(\xi^L_{\chi^\pm_i}\leftrightarrow\xi^R_{\chi^\pm_i}),\\
&\frac{G_F}{\sqrt{2}}C^d_{8G}(\Lambda) = -i\Lambda^{-2}(V^*_{ts}V_{tb})^{-1}\left\{(\eta^L_{X^j})^\dagger_{sb'}(\eta^L_{X^j})_{b'b}F^{(d)}_{1,g}(x_{b'},x_{X^j}) + \frac{m_f}{m_b}(\eta^L_{X^j})^\dagger_{sb'}(\eta^R_{X^j})_{b'b}F^{(d)}_{2,g}(x_{b'},x_{X^j})\right\},\\
&\frac{G_F}{\sqrt{2}}\tilde{C}^d_{8G}(\Lambda) = \frac{G_F}{\sqrt{2}}C^d_{8G}(\Lambda)(\eta^L_{X^j}\leftrightarrow\eta^R_{X^j}),\\
&\frac{G_F}{\sqrt{2}}C^e_{8G}(\Lambda) = -i\Lambda^{-2}(V^*_{ts}V_{tb})^{-1}\left\{(\xi^L_{\tilde{b}'})^\dagger_{s\tilde{X}^j}(\xi^L_{\tilde{b}'})_{\tilde{X}^jb}F^{(e)}_{1,g}(x_{\tilde{X}^j},x_{\tilde{b}'}) + \frac{m_f}{m_b}(\xi^L_{\tilde{b}'})^\dagger_{s\tilde{X}^j}(\xi^R_{\tilde{b}'})_{\tilde{X}^jb}F^{(e)}_{2,g}(x_{\tilde{X}^j},x_{\tilde{b}'})\right\},\\
&\frac{G_F}{\sqrt{2}}\tilde{C}^e_{8G}(\Lambda) = \frac{G_F}{\sqrt{2}}C^e_{8G}(\Lambda)(\xi^L_{\tilde{b}'}\leftrightarrow\xi^R_{\tilde{b}'})),
\end{aligned}
\tag{23}
$$

with the form factors listed below. As gluon can only be attached to intermediate fermion u_i and b' in Figure 1.(a) and 1.(d), so the form factors have the same expressions. While in Figure 1.(b), 1.(c) and Figure 1.(e), the gluon can only be attached to scalar particles. Then form factors associated to these diagrams are the same. By summing over the contributions to Wilson coefficients when gluon attached to Λ_G and $\tilde{D}$, we get form factors of Figure 1.(f).

$$
\begin{aligned}
&F^{(a)}_{1,g}(x,y) = F^{(d)}_{1,g}(x,y) = \left[-\frac{1}{24}\frac{\partial^3\varrho_{3,1}}{\partial^3 y} + \frac{1}{4}\frac{\partial^2\varrho_{2,1}}{\partial^2 y} - \frac{1}{4}\frac{\partial\varrho_{1,1}}{\partial y}\right](x,y),\\
&F^{(a)}_{2,g}(x,y) = F^{(d)}_{2,g}(x,y) = \left[-\frac{1}{4}\frac{\partial^2\varrho_{2,1}}{\partial^2 y} + \frac{1}{2}\frac{\partial\varrho_{1,1}}{\partial y} - \frac{1}{2}\frac{\partial\varrho_{1,1}}{\partial x}\right](x,y),\\
&F^{(b)}_{1,g}(x,y) = F^{(c)}_{1,g}(x,y) = F^{(e)}_{1,g}(x,y) = \left[\frac{1}{24}\frac{\partial^3\varrho_{3,1}}{\partial^3 y} - \frac{1}{8}\frac{\partial^2\varrho_{2,1}}{\partial^2 y}\right](x,y),\\
&F^{(b)}_{2,g}(x,y) = F^{(c)}_{2,g}(x,y) = F^{(e)}_{2,g}(x,y) = \left[\frac{1}{4}\frac{\partial^2\varrho_{2,1}}{\partial^2 y} - \frac{1}{2}\frac{\partial\varrho_{1,1}}{\partial y}\right](x,y),\\
&F^{(f)}_{1,g}(x,y) = \left[\frac{1}{8}\frac{\partial^2\varrho_{2,1}}{\partial^2 y} - \frac{1}{4}\frac{\partial\varrho_{1,1}}{\partial y}\right](x,y),\\
&F^{(f)}_{2,g}(x,y) = \left[-\frac{1}{2}\frac{\partial\varrho_{1,1}}{\partial x}\right](x,y).
\end{aligned}
\tag{24}
$$

The Wilson coefficients obtained above can also be used to direct CP-violation in $\bar{B}\to X_s\gamma$ and the time-dependent CP-asymmetry in $B\to K^*\gamma$. The direct CP-violation $A^{CP}_{\bar{B}\to X_s\gamma}$ and CP-asymmetry $S_{K^*\gamma}$ are defined in hadronic scale [26-30]

$$
\begin{aligned}
A^{CP}_{\bar{B}\to X_s\gamma} &= \left.\frac{\Gamma(\bar{B}\to X_s\gamma)-\Gamma(B\to X_{\bar{s}}\gamma)}{\Gamma(\bar{B}\to X_s\gamma)+\Gamma(B\to X_{\bar{s}}\gamma)}\right|_{E_\gamma>(1-\delta)E^{max}_\gamma}\\
&\simeq \frac{10^{-2}}{|C_7(\mu_b)|^2}\Big[1.23\Im(C_2(\mu_b)C^*_7(\mu_b))\\
&\quad -9.52\Im(C_8(\mu_b)C^*_7(\mu_b))\\
&\quad +0.01\Im(C_2(\mu_b)C^*_8(\mu_b))\Big],
\end{aligned}
\tag{25}
$$

$$
S_{K^*\gamma} \simeq \frac{2\mathrm{Im}(e^{-i\phi_d}C_7(\mu_b)C'_7(\mu_b))}{|C_7(\mu_b)|^2+|C'_7(\mu_b)|^2},
\tag{26}
$$

where the photon energy cut in A^{CP} is taken as $\delta = 3$, and ϕ_d in $S_{K^*\gamma}$ is phase of B_d mixing amplitude. Here we use the experimental data $\sin\phi_d = 0.67\pm0.02$ given in ref. [31].

As the Wilson coefficients are calculated at electroweak scale μ_{EW}, we need to evolve them down to hadronic scale $\mu\sim m_b$ with renormalization group equations.

$$\vec{C}_{NP}(\mu) = \hat{U}(\mu,\mu_0)\vec{C}_{NP}(\mu_0),$$
$$\vec{C}'_{NP}(\mu) = \hat{U}'(\mu,\mu_0)\vec{C}'_{NP}(\mu_0), \tag{27}$$

where the Wilson coefficients are constructed as

$$\vec{C}^{\rm T}_{NP} = (C_{1,NP},\cdots,C_{6,NP},C^{eff}_{7,NP},C^{eff}_{8,NP}),$$
$$\vec{C}'^{,\rm T}_{NP} = (C'^{eff}_{7,NP},C'^{eff}_{8,NP}). \tag{28}$$

The evolving matrices involved in Eq.(27) are given as

$$\hat{U}(\mu,\mu_0) \simeq 1 - \left[\frac{1}{2\beta_0}\ln\frac{\alpha_s(\mu)}{\alpha_s(\mu_0)}\right]\hat{\gamma}^{(0)T},$$
$$\hat{U}'(\mu,\mu_0) \simeq 1 - \left[\frac{1}{2\beta_0}\ln\frac{\alpha_s(\mu)}{\alpha_s(\mu_0)}\right]\hat{\gamma}'^{(0)T}, \tag{29}$$

with anomalous dimension matrices

$$\hat{\gamma}^{(0)} = \begin{pmatrix} -4 & \frac{8}{3} & 0 & -\frac{2}{9} & 0 & 0 & -\frac{208}{243} & \frac{173}{162} \\ 12 & 0 & 0 & \frac{4}{3} & 0 & 0 & \frac{416}{81} & \frac{70}{27} \\ 0 & 0 & 0 & -\frac{52}{3} & 0 & 2 & -\frac{176}{81} & \frac{14}{27} \\ 0 & 0 & -\frac{40}{9} & -\frac{100}{9} & \frac{4}{9} & \frac{5}{6} & -\frac{152}{243} & -\frac{587}{162} \\ 0 & 0 & 0 & -\frac{256}{3} & 0 & 20 & -\frac{6272}{81} & \frac{6596}{27} \\ 0 & 0 & -\frac{256}{9} & \frac{56}{9} & \frac{40}{9} & -\frac{2}{3} & \frac{4624}{243} & \frac{4772}{81} \\ 0 & 0 & 0 & 0 & 0 & 0 & \frac{32}{3} & 0 \\ 0 & 0 & 0 & 0 & 0 & 0 & -\frac{32}{9} & \frac{28}{3} \end{pmatrix}, \tag{30}$$

and

$$\hat{\gamma}'^{(0)} = \begin{pmatrix} \frac{32}{3} & 0 \\ -\frac{32}{9} & \frac{28}{3} \end{pmatrix}. \tag{31}$$

As the renormalization group evolution of new physics contributions can be performed independently from the SM [32], we evolved the new physics contributions from electroweak scale to hadronic scale separately. Then the complete result of Wilson coefficients at hadronic scale are obtained by adding the SM parts denoted by $C^{eff}_{7\gamma}, C^{eff}_{8g}$. To get a result as accurate as possible, we adopt the NNLO result from SM in our numerical analysis, $C^{eff}_7(m_b) = -0.304, C^{eff}_8(m_b) = -0.167$.

IV. NUMERICAL ANALYSIS

The consistency of SM prediction and experimental data on $\bar{B} \to X_s\gamma$ sets stringent constraint on new physics parameters. In this section, we discuss the numerical results of branching ratio with some assumptions. The SM inputs are given in Table 2. All the parameters with mass dimension are given in the unit GeV. To be concise, we omit all the unit GeV in this section.

As we know, the heaver new particles appearing in inner lines are, the lower it contribute to Wilson Coefficient that we need. Besides, new particles with too heavy mass are not favorite because it is difficulty to reach on the nowadays colliders. On the other hand, no signal of new particles has been observed by now. Thus the masses of exotic particles have to be heaver than a few of TeV. Based on previous study on mass spectrum in BLMSSM in [14], the parameters introduced in BLMSSM are set as $A_{BU} = A_{BD} = A_{BQ} = A'_{BU} = A'_{BD} = A'_{BQ} = A_{d_4} = A_{d_5} = A_{u_4} = A_{u_5} = A'_{d_4} = A'_{d_5} = A'_{u_4} = A'_{u_5} = 100$, $M^2_{\tilde{Q}_4} = M^2_{\tilde{Q}_5} = M^2_{\tilde{U}_4} = M^2_{\tilde{U}_5} = M^2_{\tilde{D}_4} = M^2_{\tilde{D}_5} = 2500$, $m_1 = m_2 = 1200$ and $m_{Z_B} = 1000$ to make sure the masses of new physics particles under experimental limitations. With the above setups, one can scan the other sensitive parameters with masses of new particles around a few TeV as a condition in the numerical program.

As a new field introduced in BLMSSM, superfield X interacts with exotic quarks. The coplings between X and $\hat{Q}_5, \hat{U}_5$ denoted by $\lambda_i, (i = 1,2,3)$ are given in Eq.4. From the analytical expressions, one can find the Wilson coefficients are sensitive to these couplings as well as coefficients of mass term of X, which turns up in $\mathcal{W}_X$ as μ_X and B_X. We show the branching ratio varying with λ_1, λ_3, μ_X and B_X in firgure 2. The dependency of λ_2 is not listed as it is similar to λ_1.

In Figure 2.(a), one can find the branching ratio increases when λ_1 raises up. The experimental limitations are denoted by the gray area, and we have taken $\lambda_3/(4\pi) = 0.07, \tan\beta = 10, \lambda_Q = 0.7, \lambda_U = 0.3, \lambda_D = 0.2, \mu = -600, \mu_B = m_{Z_B} = m_B = 1000, \mu_X = 1100, B_X = 400, v_{bt} = 6000$. It can be seen in this figure that branching ratio reachs the upper limitations of experimental limitations when $\lambda_1/(4\pi) = 0.95$, then we get the constrain $\lambda_1/(4\pi) < 0.95$.

Similarly, we plot the branching ratio varying with λ_3 in Figure 2.(b). By taking $\lambda_1/(4\pi) = 0.07$, which satisfies the limitations obtained in Figure 2.(a), and $\tan\beta = 5, \lambda_Q = 0.7, \lambda_U = 0.5, \lambda_D = 0.8, \mu = -800, \mu_B = \mu_X = 1100, m_{Z_B} = 1000, m_B = 500, B_X = 400, v_{bt} = 6000$, we find the branching ratio rises very slowly when $\lambda_3/(4\pi)$ runs from 0.01 to 1.5. The whole curve lies in the gray area, which means the branching ratio satisfies the experimental constraint under our assumptions.

To investigate the trends of $Br(\bar{B} \to X_s\gamma)$ varying with

Table 2. SM inputs in numerical analysis

α	1/128	m_W	80.385	m_Z	91.188
m_u	0.0023	m_c	1.275	m_t	173.5
m_d	0.0048	m_s	0.095	m_b	4.18

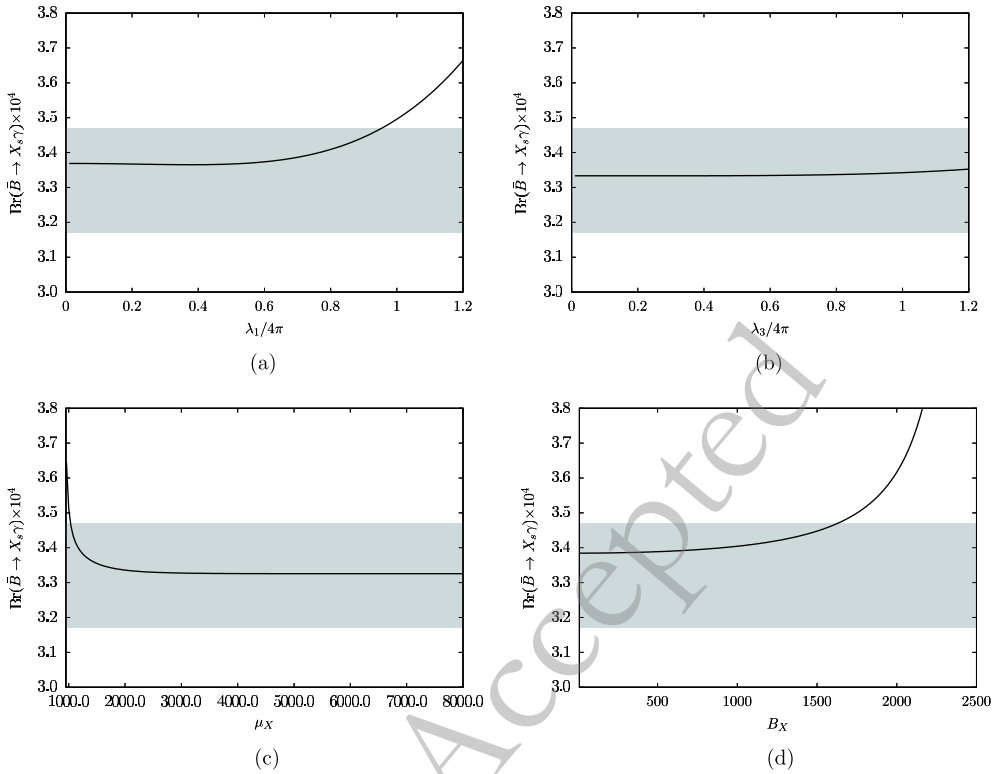

Fig. 2. $Br(\bar{B}\to X_s\gamma)$ varying with parameters relevant to superfield X

μ_X, we take $\lambda_1/(4\pi)=0.06, \lambda_3/(4\pi)=0.08, \tan\beta=5, \lambda_Q=0.8, \lambda_U=0.5, \lambda_D=0.2, \mu=-600, \mu_B=1000, B_X=400, m_{z_B}=1100, v_{bt}=6000, m_B=2500$. We find from Figure 2.(c) that the branching ratio diminishes steeply with increasing of μ_X, and finally gets to the value of standard model. In Figure 2.(d), we plot the branching ratio varying with B_X, where we take $\lambda_1/(4\pi)=0.15, \lambda_3/(4\pi)=0.08, \tan\beta=5, \lambda_Q=0.7, \lambda_U=0.2, \lambda_D=0.3, \mu=-1000, \mu_B=1100, \mu_X=2500, m_{z_B}=900, v_{bt}=5500, m_B=2000$. With the upper limitations of experimental result, we get the constraints $B_X<1625$.

In Figure 3.(a), we present the branching ratio varying with λ_Q, which is the coupling truns up in superpotential term $\lambda_Q\hat{Q}_4\hat{Q}_5^c\hat{\Phi}_B$. With $\lambda_1/(4\pi)=0.08, \lambda_3/(4\pi)=0.06, \tan\beta=20, \lambda_U=0.3, \lambda_D=0.6, \mu=-800, \mu_B=1000, \mu_X=1200, B_X=400, m_{z_B}=1000, v_{bt}=5000, m_B=1500$, we find branching ratio decreases when λ_Q gets larger. To consist with the experimental data, one has $\lambda_Q>0.62$. Another interesting parameter is v_{bt}, which is defined as $v_{bt}=\sqrt{\bar{v}_B^2+v_B^2}$, where v_B and $\bar{v}_B$ are VEVs of Φ_B and φ_B respectively. We plot branching ratio varying with v_{bt} in Figure 3.(b) with $\lambda_1/(4\pi)=\lambda_3/(4\pi)=0.1, \tan\beta=5, \lambda_Q=0.7, \lambda_U=0.2, \lambda_D=0.7, \mu=-1000, \mu_B=1100, \mu_X=1400, B_X=400, m_{z_B}=1000, m_B=1500$. To satisfy the experimental constraints, we have $v_{bt}>4200$.

Additionally, we plot the direct CP-violation of $\bar{B}\to X_s\gamma$ and time-dependent CP-asymmetry of $B\to K^*\gamma$ varying with $\lambda_1, \lambda_3, \mu_X, B_X, \lambda_Q, \lambda_D$ and v_{bt}. Within the framework of SM, we have $-0.6\%<A_{CP}^{SM}<+2.8\%$ [33], and the average value of this observable is $A_{CP}^{exp}=-0.009\pm0.018$[35,34]. Within some uncertainty, the theoretical value is consistent with the experimental result. Compared with direct CP-violation of $\bar{B}\to X_s\gamma$, there is significant deviation between SM prediction and experimental result of $S_{K^*\gamma}$. The SM prediction of time-dependent CP-asymmetry in $B\to K^*\gamma$ at LO level is given as $S_{K^*\gamma}^{SM}\simeq(-2.3\pm1.6)\%$ [36] and the experimental result is $S_{K^*\gamma}\simeq-0.15\pm0.22$ [34].

To investigate $A_{\bar{B}\to X_s\gamma}^{CP}$ and $S_{K^*\gamma}$ numerically, some parameters are taken to be complex, and the area within experimental boundaries are filled to be gray in the presented figures. In Figure 4, we plot the dependency of parameters relevant to superfield X. Under our assumptions of free parameters introduced in BLMSSM, we find that $A_{\bar{B}\to X_s\gamma}^{CP}$ (solid line) are hardly affected by the change of $\lambda_1, \lambda_3, \mu_X, B_X$. Though corrections from one-loop level are almost zero, the numerical results are consistent with experimental data.

As shown in Figure 4.(a), one-loop corrections to $S_{K^*\gamma}$ (dashed line) in BLMSSM can reach -0.25 with appropriate inputs. By changing the free parameters, one finds $S_{K^*\gamma}$ can be as small as zero in Figure 4.(b). In Figure 4.(c), it can be seen that $S_{K^*\gamma}$ raise obviously with increasing of μ_X, and finally gets stable around zero. The $S_{K^*\gamma}$ varying with B_X are given in Figure 4.(d). When B_X raises up, we can see that $S_{K^*\gamma}$ decreases. Within the

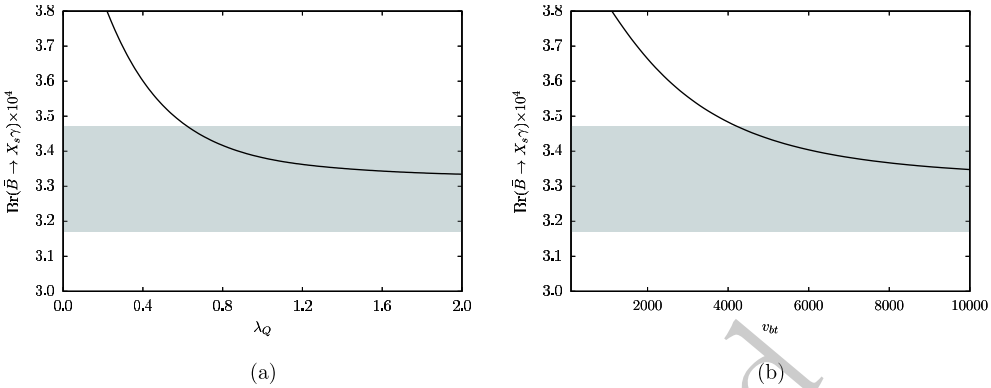

Fig. 3. $Br(\bar{B} \to X_s\gamma)$ varying with λ_Q and v_{bt}

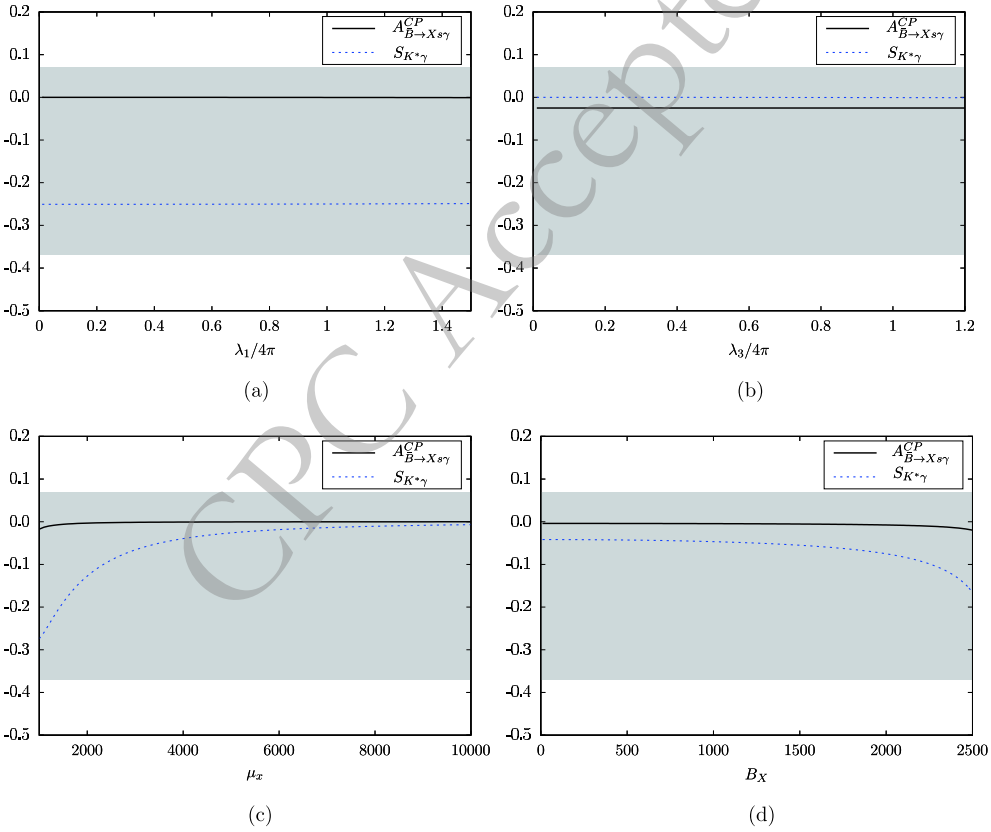

Fig. 4. $A^{CP}_{\bar{B}\to X_s\gamma}$ and $S_{K^*\gamma}$ varying with paremeters relevant to superfield X

range of parameters $\lambda_1, \lambda_3, \mu_X$ and B_X, we find $S_{K^*\gamma}$ is consistent with experimental data.

In Figure 5, we take into account the parameters λ_Q and λ_D. When λ_Q runs from 0.01 to 2.0, the time-dependent CP-asymmetry decrease from 0.02 to −0.22. While for the increasing of λ_D, $S_{K^*\gamma}$ raises from −0.28 to −0.02. Under our assumptions, we conclude that λ_Q and λ_D affect $S_{K^*\gamma}$ apparently, and the numerical results of new physics correction are consistent with experimental data. However, the direct CP-violation of $\bar{B} \to X_s\gamma$ depends on λ_Q and λ_D weakly, and the one-loop contributions from BLMSSM are very small.

The last Figure 6 illustrates the trend of $S_{K^*\gamma}$ and $A^{CP}_{\bar{B}\to X_s\gamma}$ varying with v_{bt}. By taking $\lambda_1/(4\pi) = 0.8, \lambda_3/(4\pi) = 0.9, B_X = 400$ and $\lambda_Q = 0.4e^{0.625\pi}$, we find that $S_{K^*\gamma}$ increases from −0.26 to −0.06. The $A^{CP}_{\bar{B}\to X_s\gamma}$ stays around zero within the range $100 < v_{bt} < 10000$.

To analyze the dependence of Wilson coefficients and CP-asymmetry on the scale μ_b, numerical results of $C^{NP}_{7,8}$, $\tilde{C}^{NP}_{7,8}$, A_{CP} and $S_{K^*\gamma}$ are given in Table 3. The input parameters are the same as in Figure 5.(b) with $\lambda_D = 0.1$. It can be seen that the CP violation/asymmetry get more significant when μ_b become lager. By printing the coeffi-

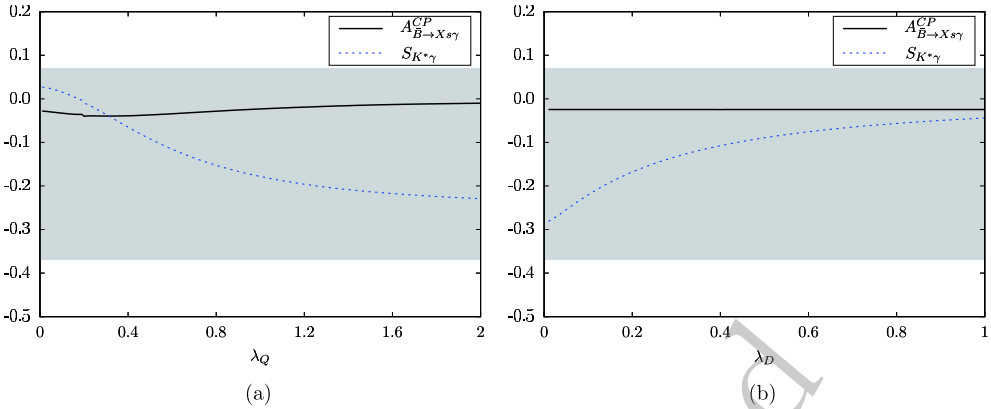

Fig. 5. $A^{CP}_{\bar{B}\to X_s\gamma}$ and $S_{K^*\gamma}$ varying with λ_Q and λ_D

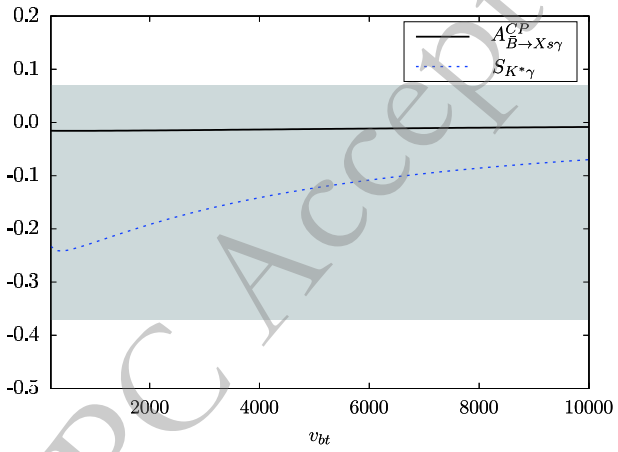

Fig. 6. $A^{CP}_{\bar{B}\to X_s\gamma}$ and $S_{K^*\gamma}$ varying with v_{bt}

Table 3. Dependence of $C^{NP}_{7,8}$, $\tilde{C}^{NP}_{7,8}$, A_{CP} and $S_{K^*\gamma}$ on typical scales

μ_b	$\lvert C^{NP}_7\rvert$	$\lvert C^{NP}_8\rvert$	$\lvert \tilde{C}^{NP}_7\rvert$	$\lvert \tilde{C}^{NP}_8\rvert$	A_{CP}	$S_{K^*\gamma}$
$m_b/2 = 2.09$ GeV	0.078	0.013	0.053	0.014	−0.019	−0.200
$m_b = 4.18$ GeV	0.100	0.016	0.067	0.017	−0.025	−0.220
$2m_b = 8.36$ GeV	0.118	0.018	0.078	0.020	−0.028	−0.228

cients from different diagrams seperately, one can find the dominant corrections come from Figure 1.(e), which contains exotic squark charged -1/3 and superfield $\tilde{X}$.

V. CONCLUSIONS

As an interesting process of FCNC, we investigate the transition $b \to s\gamma$ within the framework of BLMSSM. With effective Hamiltonian method, we present the Wilson coefficients extracted from amplitudes corresponding to the concerned one-loop diagrams. Based on the analytical expressions, constraints on parameters are given in the numerical section with the experimental data of branching ratio of $\bar{B} \to X_s\gamma$. The direct CP-violation of $\bar{B} \to X_s\gamma$ in BLMSSM is very small, and depend on the free parameters weakly. However, the time-dependent CP-asymmetry $S_{K^*\gamma}$ in $B \to K^*\gamma$ varies with $\mu_X, B_X, \lambda_Q, \lambda_D$ and v_{bt} obviously. The contributions from new physics can reach −0.28 under appropriate setup of the parameters.

References

[1] Y. Amhis et al. (Heavy Flavor Averaging Group Collaboration), arXiv: 1909.12524[hep-ex]
[2] M. Misiak, *et al.*, Phys. Rev. Lett. **114**, 221801 (2015)
[3] M. Czakon, P. Fiedler, T. Huber, M. Misiak, T. Schutzmeier and M. Steinhauser, (2015), arXiv: 1503.01791[hep-ph]
[4] M. Misiak, Abdur Rehman, JHEP(2020), 175 (2006)

[5] H. P. Nilles, Phys. Rept. **110**, 1 (1984)
[6] H. E. Haber and G. L. Kane, Phys. Rep. **117**, 75 (1985)
[7] J. Rosiek, Phys. Rev. D **41**, 3464 (1990)
[8] P. F. Perez and M. B. Wise, JHEP **1108**, 068 (2011)
[9] P. F. Perez and M. B. Wise, Phys. Rev. D **82**, 011901 (2010)
[10] P. F. Perez, Physics reports **597**, 1 (2015)
[11] S. M. Zhao, T.F. Feng, H.B.Zhang, B. Yan and Y. J. Zhang, JHEP **1411**, 119 (2014)
[12] S. M. Zhao, T. F. Feng, Z, J. Yang, H. B. Zhang, X. X. Dong and T. Guo, Eur. Phys. J. C **102**, 77 (2017)
[13] T. F. Feng, S. M. Zhao, H. B. Zhang, Y. J. Zhang, Y. L. Yan, Nucl. Phys. B **871**, 223 (2013)
[14] H. Li, J. B. Chen and L. L. Xing, MPLA **33**, 1850034 (2018)
[15] E. Lunghi and J. Matias, JHEP **0704**, 058 (2007)
[16] G. Buchalla, A. J. Buras and M. E. Lautenbacher, Rev. Mod. Phys. **68**, 1125 (1996)
[17] T. F. Feng, Y. L. Yan, H. B. Zhang and S. M. Zhao, Phys. Rev. D **92**, 055024 (2015)
[18] C. Bobeth, M. Misiak and J. Urban, Nucl. Phys. B **574**, 291-330 (2000)
[19] W. Altmannshofer, P. Ball1, A. Bharucha, A. J. Buras, D. M. Straub1 and M. Wick, JHEP **01**, 019 (2009)
[20] R. Grigjanis, P.J. ODonnell, M. Sutherland, H. Navelet, Phys. Rep. **22**, 93 (1993)
[21] W. Altmannshofer, P. Ball, A. Bharucha, A.J. Buras, D.M. Straub and M. Wick, JHEP **0901**, 019 (2009)
[22] P. Goertz, T. Pfoh, Phys. Rev. D **84**, 095016 (2011)
[23] T. F. Feng, X. Q. Li and G. L. Wang, Phys. Rev., D **65**, 055007 (2002)
[24] N. G. Deshpande, M. Nazerimonfared, Nucl. Phys, B **213**, 390 (1983)
[25] M. Ciuchini, G. Degrassi, P. Gambino and G.F. Giudice, Nucl. Phys, B **527**, 21 (1998)
[26] H. M. Asatrian and A. N. Ioannissian, Phys. Rev. D **54**, 5642 (1996)
[27] M. Ciuchini, E. Gabrielli and G.F. Giudice, Phys. Lett. B **388**, 353 (1996)
[28] S. Baek, P. Ko, Phys. Rev. Lett. **83**, 488 (1999)
[29] A. L. Kagan and M. Neubert, Phys. Rev. D **58**, 094012 (1998)
[30] K. Kiers, A. Soni, and G. H. Wu, Phys. Rev. D **62**, 116004 (2000)
[31] D. Asner et al.(Heavy Flavor Averaging Group), (2010) arXiv: 1010.1589[hep-ex]
[32] A. J. Buras, L. Merlo and E. Stamou, JHEP **1108**, 124 (2011)
[33] M. Benzke, S. J. Lee, M. Neubert and G. Paz, Phys. Rev. Lett. **106**, 141801 (2011)
[34] P.A. Zyla, *et al.*, Prog. Theor. Exp. Phys. **2020**, 083C01 (2020)
[35] S. Watanuki (Belle Collaboration), Phys. Rev. D **99**, 032012 (2019)
[36] P. Ball, G. W. Jones and R. Zwicky, Phys. Rev. D **75**, 054004 (2007)